Supplementary Information

Adjusting Molecular Weight Optimizes Electronic Transport of Extrinsically N-type Doped Conjugated Polymer Entailing Glycolated Side Chains

Yazhuo Kuang,[ab] Sander Heester,[d] Shuyan Shao[c], Gang Ye,[a] Tangqin Yao,[ab] Zhiyuan Xie,[ab] L. Jan Anton Koster[d] and Jian Liu[ab]

a. *State Key Laboratory of Polymer Physics and Chemistry, Changchun Institute of Applied Chemistry, Chinese Academy of Sciences, Changchun 130022 (P. R. China). E-mail: jian.liu@ciac.ac.cn; g.ye0612@ciac.ac.cn; xiezy_n@ciac.ac.cn*

b. *School of Applied Chemistry and Engineering, University of Science and Technology of China, Hefei 230026 (P. R. China)*

c. *Institute of Molecular Aggregation Science, Tianjin University, Tianjin 300072, China*

d. *Zernike Institute for Advanced Materials, University of Groningen, Nijenborgh 4, NL-9747 AG, Groningen, The Netherlands*

Contents

Synthesis and Characterization of Materials

Reagents: All reagents and solvents were commercial and were used as received. 2,6-dibromo-1,4,5,8-naphthalene tetracarboxylic diimide was purchased from Derthon Optoelectronics Materials Science Technology CoLTD (Shen Zhen). 4,4'-bis(octyloxy)-2,2'-bis(trimethylstannyl)-5,5'-bithiazole (2Tz) was purchased from Suna Tech. 2-(2-(2-mthoxyethoxy)ethoxy)ethanamine and bis(2-(2-(2-ethoxyethoxy)ethoxy)ethyl)benzo[lmn][3,8]phenanthroline-1,3,6,8(2H,7H)-tetraone (NDI-3O) were synthesized according to literature procedures S1-S2.

Characterization: GPC measurements were done on a GPC-PL220 room temperature GPC/SEC system at 30 °C vs. polystyrene standards using hexafluoroisopropanol (HFIP) as eluent. Cyclic voltammetry (CV) was carried out with a CHI760 Evoltammetric potentiostat in a three-electrode configuration where the working electrode was a platinum disk electrode, the counter electrode was a platinum wire, and the pseudo-reference was an Ag/AgCl wire that was calibrated against ferrocene/ferrocenium redox (Fc/Fc+). Cyclic voltammograms for the D-A copolymer films deposited on the glassy carbon working electrode in CHCN3 solution containing Bu4NPF6 (0.1 mol L-1) electrolyte at a scanning rate of 100 mV s^{-1}.

General synthetic procedures for the NDI-2Tz based polymers: To a dry three-neck flask, NDI based monomer NDI-3O (0.1 mmol) and bithiazole based monomer 2Tz (0.1 mmol) were added under N2 followed by tris(dibenzylideneacetone) dipalladium [Pd2(dba)3] (8 mg) and tri(o-tolyl)phosphine [P(o-tolyl)3] (12 mg). The flask and its contents were subjected to 3 pump/purge cycles with N2 followed by adding anhydrous, degassed chlorobenzene (5 mL) via a syringe. The reaction mixture was stirred for different reaction times (5 min, 10 min, 6 hours, 1 day, 7 days) and temperatures (110 °C or 135 °C). After cooling to room temperature, the profoundly colored mixture was dropped into 100 mL vigorously stirred methanol (containing 5 mL 1 M hydrochloride acid). After stirring for half an hour, the precipitated solid was

collected by filtration. The solid polymers were re-dissolved in chloroform and reprecipitated into methanol. After filtration, the polymers were subjected to sequential Soxhlet extraction. The sequential solvents were methanol, hexane, and chloroform. Impurities and low-molecular-weight fractions were removed by methanol and hexane. Finally, the polymer solution in chloroform was concentrated to give the polymers a dark solid.

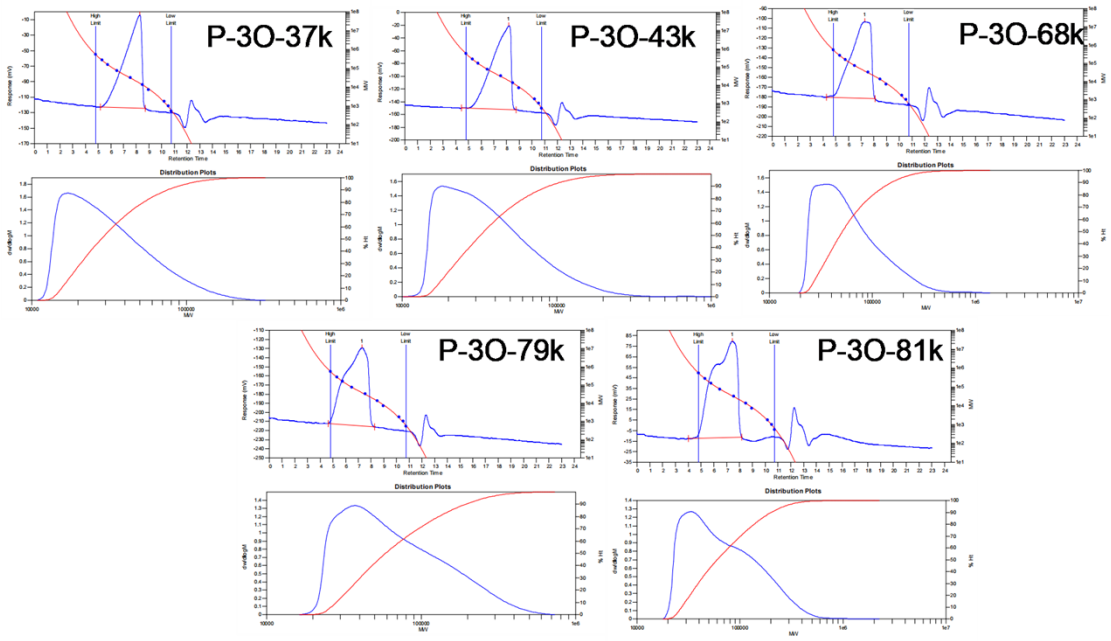

Figure S1 Gel permeation chromatography traces of P-3O with different molecular weights.

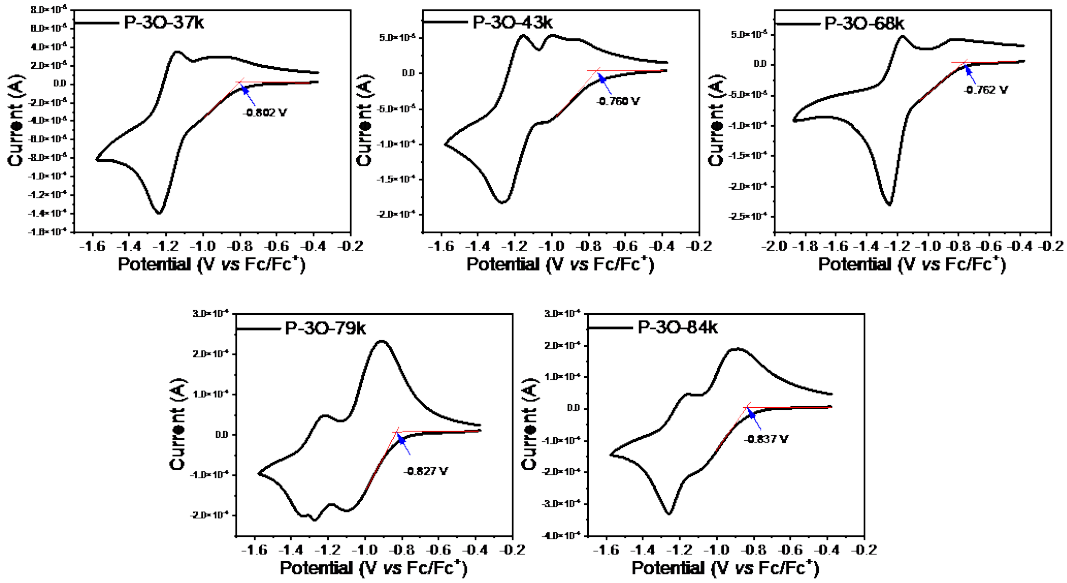

Figure S2. Cyclic voltammograms of the P-3O polymer with different thin films of molecular weight deposited on a glass carbon working electrode immersed in 0.1M n-Bu_4PF_6 acetonitrile solution at 100 mVs^{-1}.

Characterization Methods

Atomic Force Microscopy (AFM): The AFM was performed with Bruker Dimension ICON AFM in peak force mode. The sample with all batches of P-3O was prepared as film fabrication.

Grazing-Incidence Wide-Angle X-ray Scattering(GIWAXS): The GIWAXS data were obtained at 1W1A Diffuse X-ray Scattering Station, Beijing Synchrotron Radiation Facility (BSRF-1W1A). The incidence angle was performed at 0.2°. The P-3O was deposited on silicone with a thickness near 50nm.

Conductivity and Seebeck Coefficient: For electrical conductivity measurement and Seebeck coefficient measurement, which were conducted in a glove box with a nitrogen atmosphere, the parallel-shape electrodes (3nm Cr+40nm Au) were deposited at the surface of the glass before film spin-coated to form the bottom contact. The electrical conductivity σ of the four-probe measurement was measured by Keithley 2450, which self-coded LabView controlled. The σ was calculated as the following formula: $\sigma = (J/V)\times L/(w\times d)$, the channel length(L) was 3.0mm, the width of the electrode was 0.5mm, and the thickness d of the film was nearly 50-60nm. The Seebeck coefficient was determined by measuring the thermal voltage with a continuously changing temperature gradient. A set of home-made devices realized this. A Peltier element served as a temperature gradient provider. Keysight DAQ 970A measured the temperature gradient, and Keysight 973A collected the voltage difference simultaneously. The size of the electrodes was 4.0*1.2 mm^2, and the channel length of the pair was 2.8 mm. Each electrical conductivity and Seebeck coefficient were averaged by 12 devices and six devices, respectively.

Metal–Insulator–Semiconductor (MIS): MIS devices were fabricated as the reported procedure[1]. We employed admittance spectroscopy for ion-gel-based metal–insulator–semiconductor devices to extract free charge density. This technique modulates the depletion region, mainly the adjacent area between the doped semiconductor layer and dielectric layer through field effect. The whole MIS device

capacitance was measured by admittance spectroscopy. Free charge density could be obtained from Mott-Schottky analysis[2], described by the following:

$$n = \frac{2}{q\varepsilon_r\varepsilon_0 \frac{\partial C_p^{-2}}{\partial V}}$$

where ε_r and ε_0 are the dielectric constant of the active layer and vacuum, C_p is the total capacitance of the MIS devices.

For the MIS device, an architecture of ITO/Ion gel/doped P-3O/Al was adopted[1]. 202mg PVDF-HFP was dissolved in 2.55ml cyclohexanone and stirred at 70℃ overnight. 73.5mg [EMIM][TFSI] was added into the solution and stirred in 55℃ for 1h. The solution was spun and cast onto the ITO to form a ~300nm insulator layer. The wet film was annealed at 100℃ for 10min immediately and then 120℃ for three hours to get a near-transparent film. After cooling to room temperature, a mixed solution of different batches of P-3O and N-DMBI was spun, cast to the insulator, and annealed as described in the experimental section. 120nm Al were deposited onto the doped films as top electrodes. Admittance spectroscopy was measured at 50Hz with voltage varied from 0V to 2V.

Hall measurement: The hall measurement was performed by Lake Shore M91 FastHall™ in an ambient atmosphere. The hall devices were encapsulated with a smaller glass substrate on the top of the doped films. Au electrodes were routed to ensure measurement. A magnetic field intensity of 800mT was employed.

OECT testing: Glass substrates with interdigitated electrodes were prepared for the device fabrication. Five pairs of interdigitated electrodes patterned the channel between the source and drain with W/L = 1000 μm/20 μm. The polymer solutions were spun on the interdigitated electrodes, and a PDMS tank was placed onto the polymer film to confine the 0.1M NaCl solution. The Ag/AgCl electrode was the gate electrode to measure OECT performance.

Electrochemical Impedance Spectroscopy (EIS): In EIS measurement, glass slides with a layer of ITO were treated as the device fabrication. The area of P-3O film was patterned as follows: Firstly, 3nm Cr+40 nm Au were deposited onto the ITO with

variable patterned square area. Next, 2µm SU-8 was spun-cast on the patterned electrodes and went through the standard lithograph process. Then, a unique custom mask was used for light exposure to expose only the patterned Au area. The residual solidified photoresistor served as a protecting layer. Finally, the polymer solution was spun-coated on the photoresistor, and a hollow PDMS tank was attached to the polymer film to restrict 0.1M NaCl solution, which was used as an electrolyte. The patterned Au layer and P-3O attached were WE. Ag/AgCl electrode was used as RE, and a platinum wire was served as WE. For volumetric capacitance measurements, WE were set to −0.86, 0.90, 0.85, 0.80, and 0.90V with increasing Mw, corresponding to the voltage of maximum $g_{m,}$ respectively. WE were set to 0, 0.2, 0.4, 0.6, 0.8, and 1.0V to obtain the relation of capacitance voltage. The spectra were recorded in the frequency range of 0.1 Hz to 10 kHz. Zview was used to extract the capacitance by fitting the result with Equivalent Circuit: R_s+ CPE_1/R_{ct1} + CPE_2/R_{ct2}, where R_s is the active electrolyte resistance, CPE is a constant phase element, R_{ct} is the charge transfer resistance. There were two peaks in the phase-frequency plot. Thus, we modified the original model (R_s+ CPE/R_{ct}) to two CPE elements, which correlated well with our data. We assumed CPE_2 as a capacitance of gold electrode in the high-frequency region(~10^3Hz), and CPE_1 was the actual capacitance of P-3O in low frequency(0.1~10Hz).

UV-Vis-NIR absorption spectra

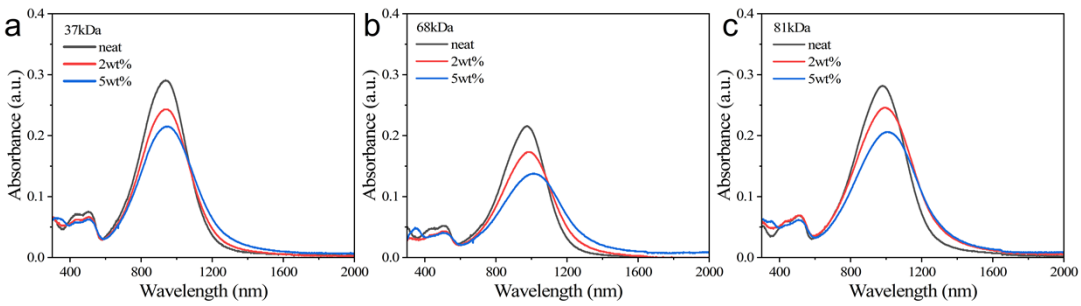

Figure S3 UV-VIS-NIR absorption spectra of neat, 2wt% and 5wt% N-DMBI doped a) 37kDa, b) 68kDa and c) 81kDa of P-3O.

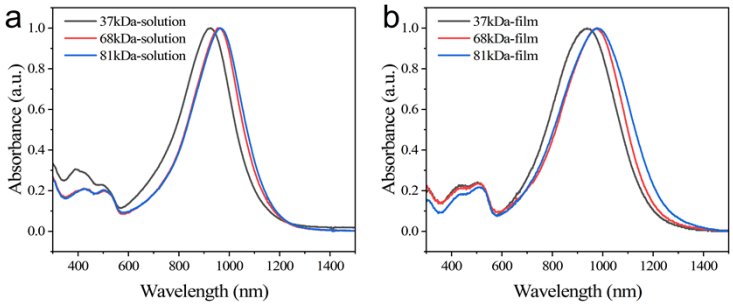

Figure S4 UV-VIS-NIR absorption spectra of P-3O with molecular weight of 37, 68 and 81kDa in a) solution and b) film.

Morphology Characterization

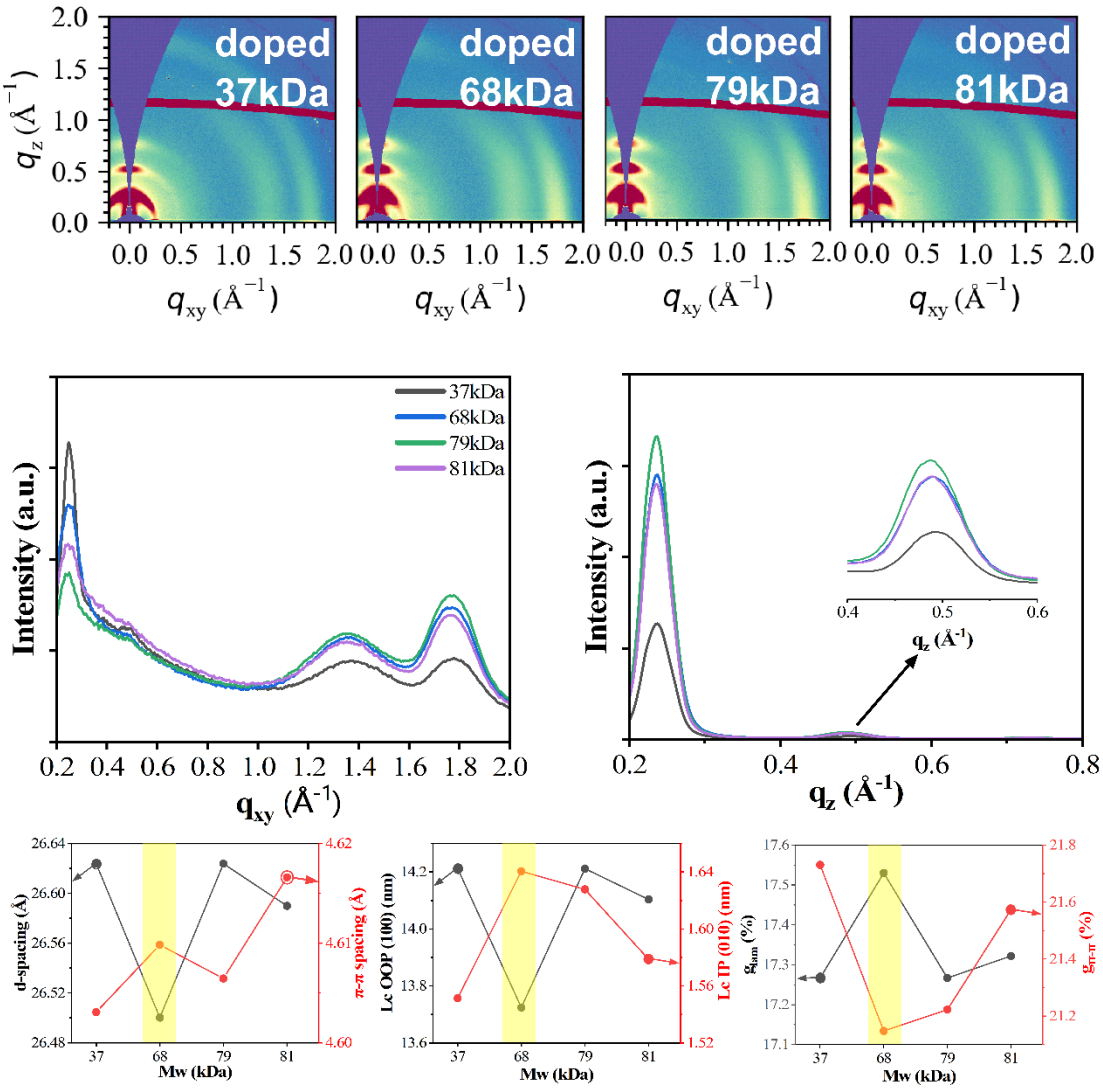

Figure S5 GIWAXS picture (above), line cuts (middle) of doped P-3O, and analysis(below).

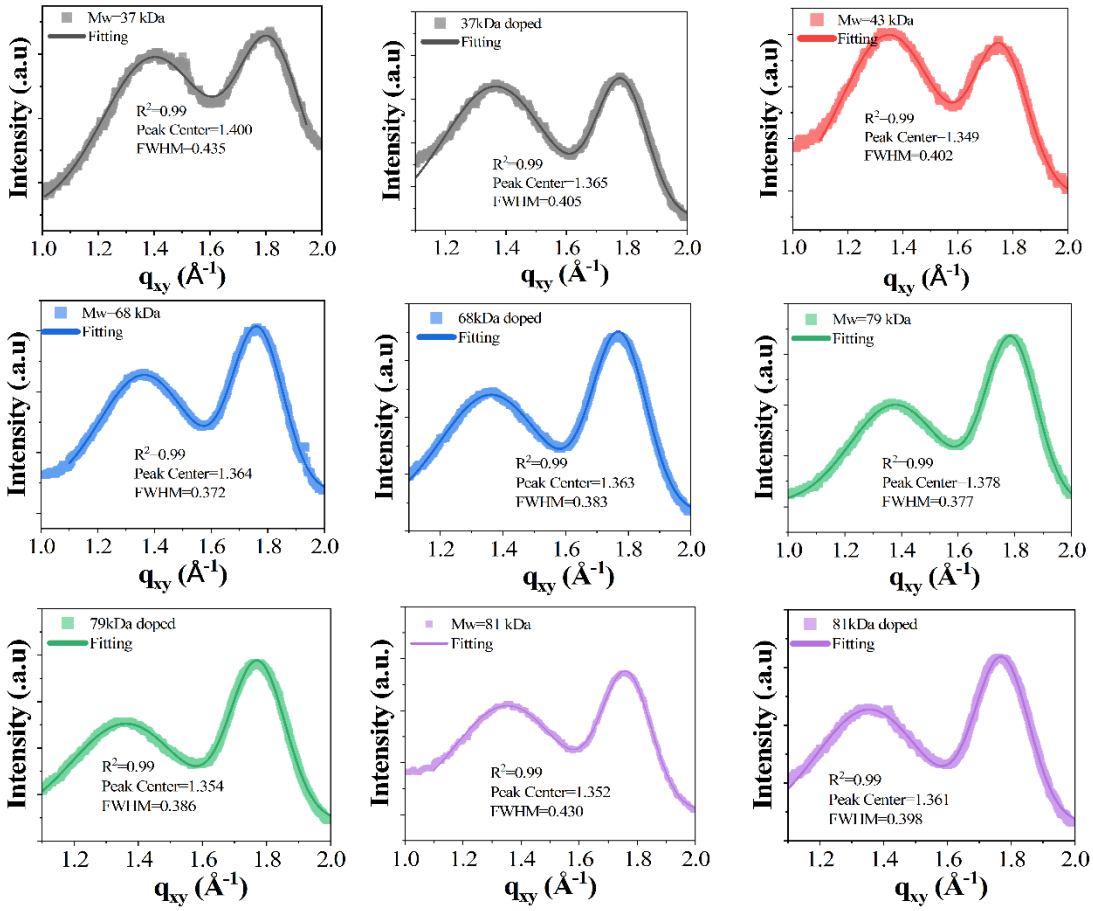

Figure S6 GIWAXS fitting data of pristine and 5wt% N-DMBI doped P-3O in the direction of in plane.

Thermoelectric Performance

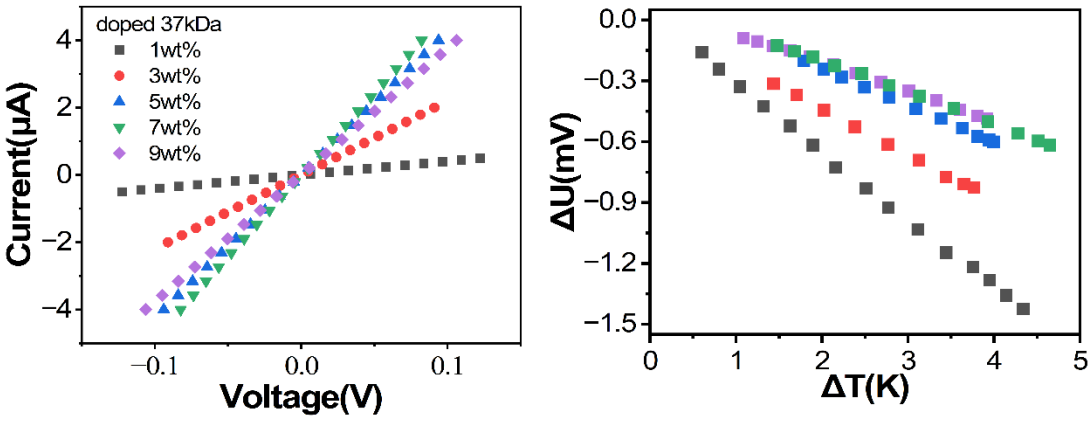

Figure S7 I-V curves of 37kDa by four probe measurement(right) and thermal voltage versus temperature

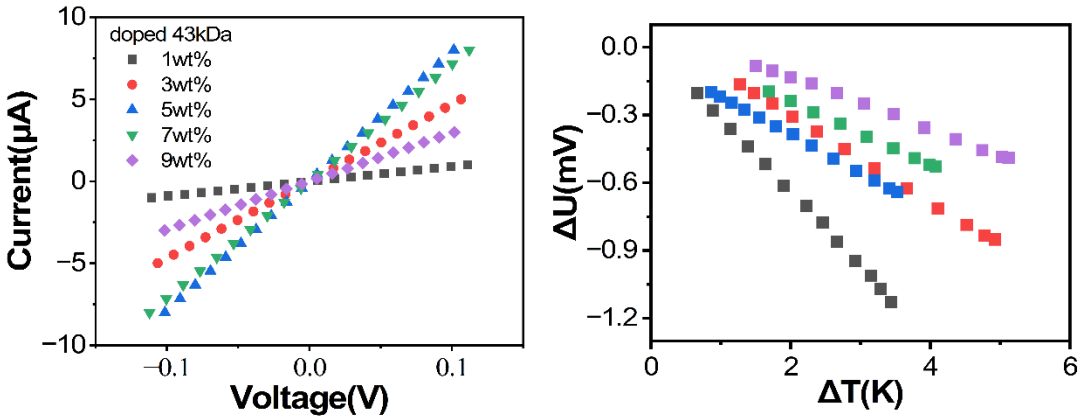

Figure S8 I-V curves of 43kDa by 4 probe measurement(right) and thermal voltage versus temperature

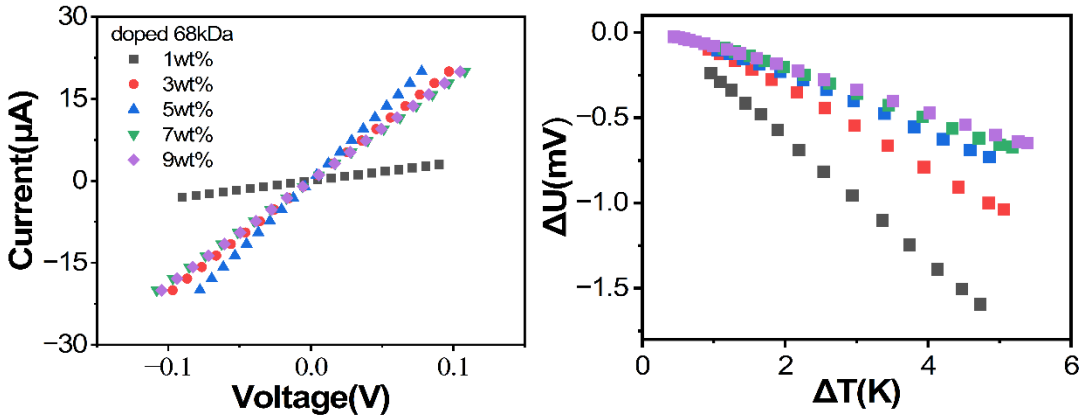

Figure S9 I-V curves of 68kDa by 4 probe measurement(right) and thermal voltage versus temperature

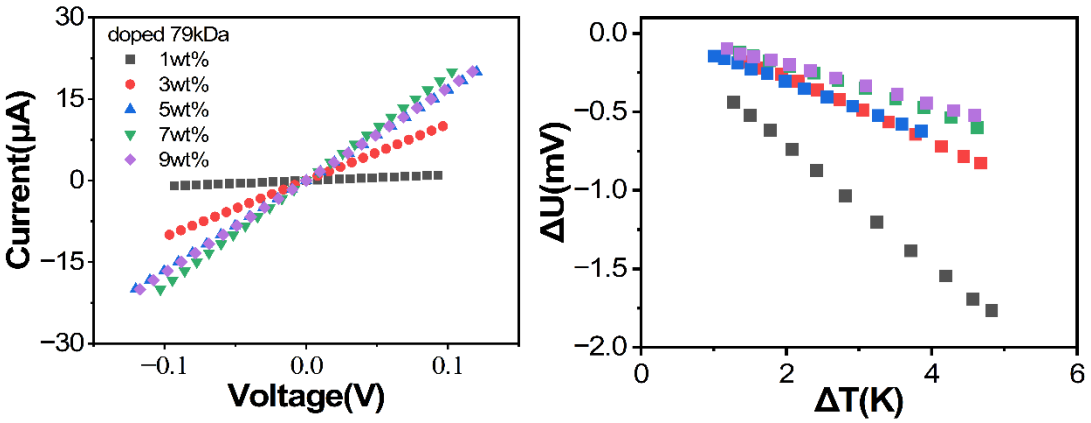

Figure S10 I-V curves of 79kDa by 4 probe measurement(right) and thermal voltage versus temperature

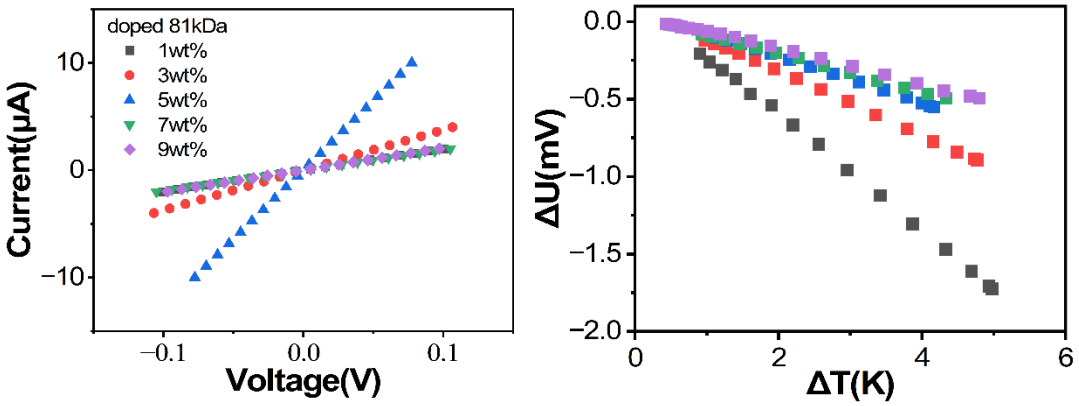

Figure S11 I-V curves of 81kDa by 4 probe measurement(right) and thermal voltage versus temperature

Kang-Snyder Model & Semi-Localized Transport (SLoT) Model

The Kang-Snyder Model and the SLoT model are based on the following expressions for the electrical conductivity σ and the Seebeck coefficient S as a function of energy *E* and temperature *T*:

$$\sigma = \int_{-\infty}^{\infty} \sigma_E(E,T)\left(-\frac{df}{dE}\right)dE$$

$$S = \frac{1}{\sigma}\left(\frac{k_b}{e}\right)\int_{-\infty}^{\infty} \sigma_E(E,T)\left(\frac{E-E_F}{k_bT}\right)\left(-\frac{df}{dE}\right)dE$$

where σ_E is the transport function, f the Fermi-Dirac distribution function, k_b the Boltzman constant, e the elementary charge and E_F the Fermi energy.

The Kang-Snyder model uses the following expression for the transport function $\sigma_E(E,T)$:

$$\sigma_E(E,T) = \sigma_{E_0}(T) \times \left(\frac{E-E_t}{k_bT}\right)^s, \quad (E > E_t)$$
$$= 0, \ (E < E_t)$$

where σ_{E0} denotes the energy independent transport coefficient, E_t is the energy of the transport edge and s is the dimensionless transport parameter.

The SLoT model uses an extended expression for the transport function $\sigma_E(E)$, taking into account the carrier concentration ratio c:

$$\sigma_E(E,T,c) = \sigma_{E_0}(T) \times e^{\left(-\frac{W_H(c)}{k_bT}\right)} \times \left(\frac{E-E_t}{k_bT}\right)^s, \quad (E > E_t)$$
$$= 0, \ (E < E_t)$$

where $W_H(c)$ is the depth of the potential energy well dependent on the carrier concentration ratio and can be expressed in a generalized form together with a semi-empirical relationship for the carrier concentration ratio:

$$W_H(c) = W_H^{max} - W_H^{slope} c^{\frac{1}{3}}, \quad (c \leq c_d)$$
$$= 0, \ (c > c_d)$$
$$c = \frac{c_{max}}{e^{\left(A_0\left(A_1 - \eta\right)\right)} + 1}$$

where c_d is the carrier ratio where delocalized transport is achieved and η the reduced fermi energy level.

Table S1 Kang-Snyder Model parameters for S-σ fits for the doped P-30 films with Mw = 37 kDa and Mw = 68 kDa.

Mw	**σ_{E0} (S/cm)**	**s**
37 kDa	1.4	1
68 kDa	10	1

Table S2 Semi-Localized Transport Model parameters for S-σ fits for the doped P-30 films with Mw = 37 kDa and Mw = 68 kDa.

Mw	**c_{max}(-)**	**A_0**	**A_1**	**$W_{h,max}$ (meV)**	**$W_{h,slope}$ (meV)**
37 kDa	0.15	1	1	1	1
68 kDa	0.14	1.2	1	1	1

OECT device

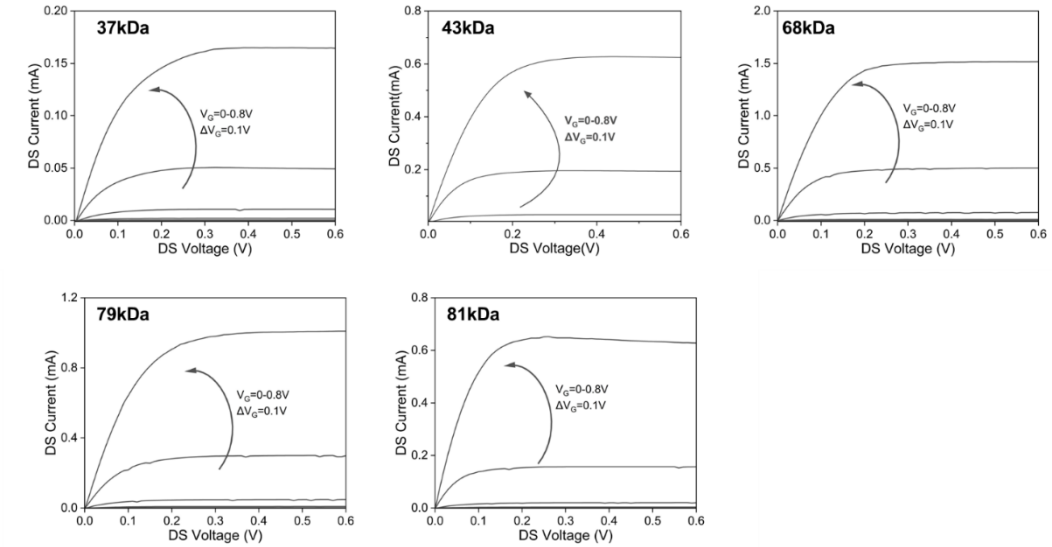

Figure S12 OECT output characteristics of all batches of P-3O

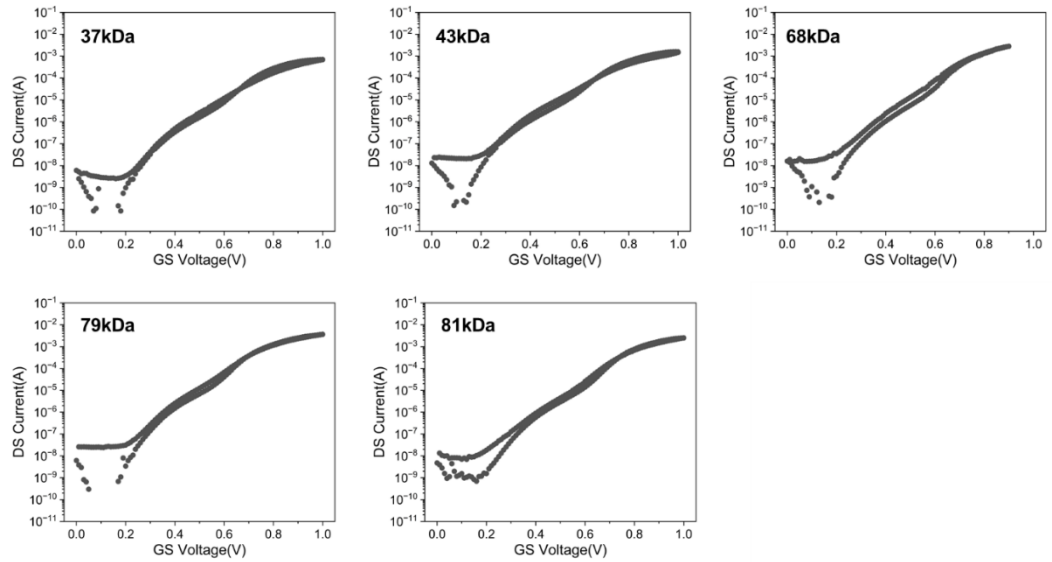

Figure S13 semi-logarithm transfer curve of all batches of P-3O

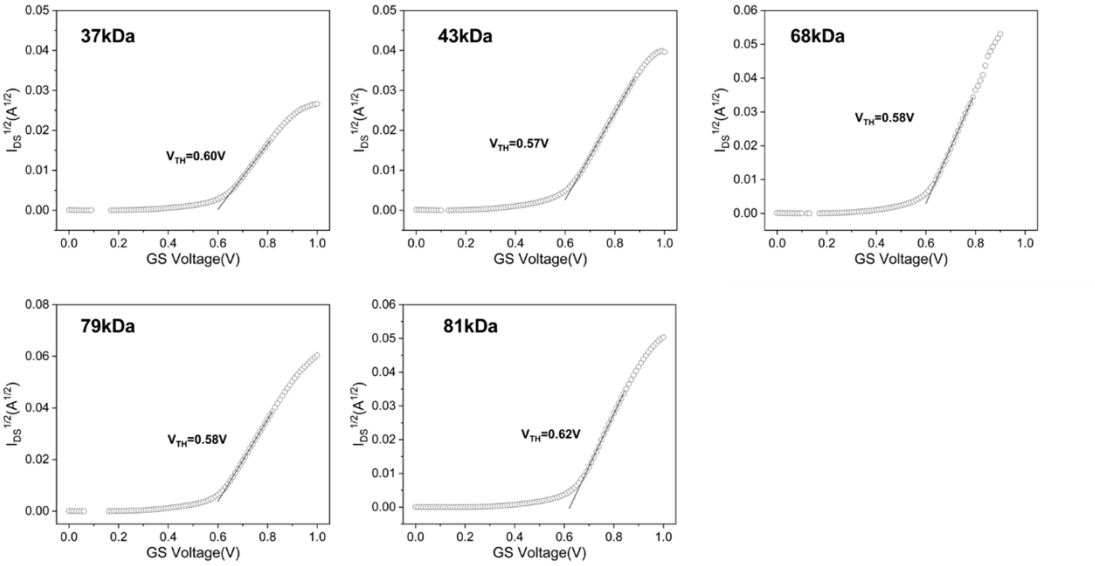

Figure S14 Threshold voltage of all batches of P-3O

Electrochemical Impedance Spectroscopy

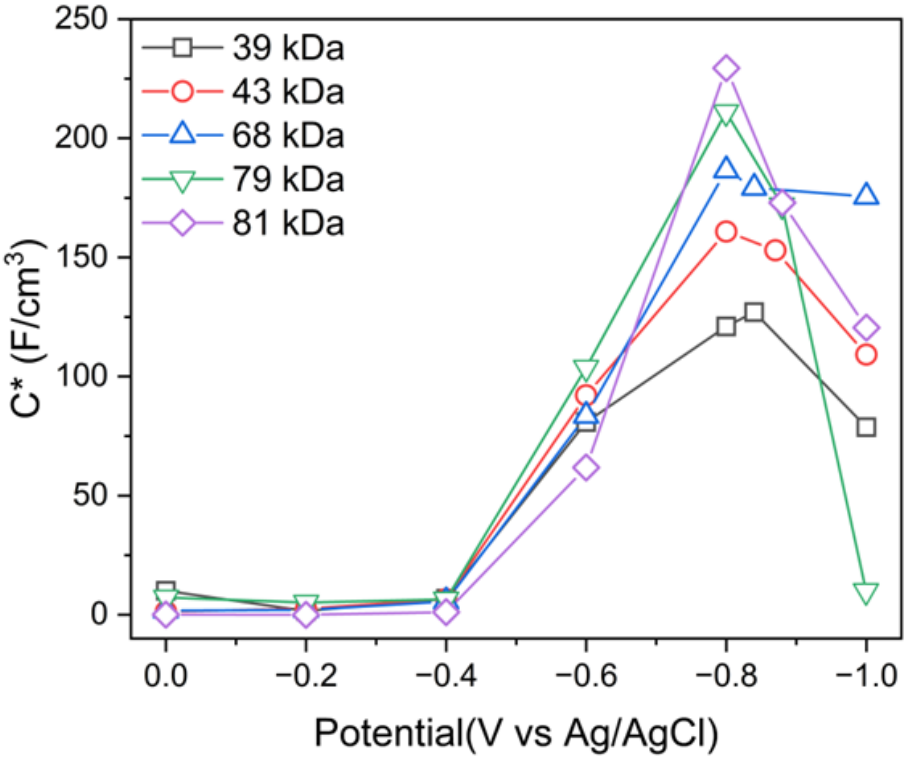

Figure S15 Volumetric capacitance of different voltage(left)

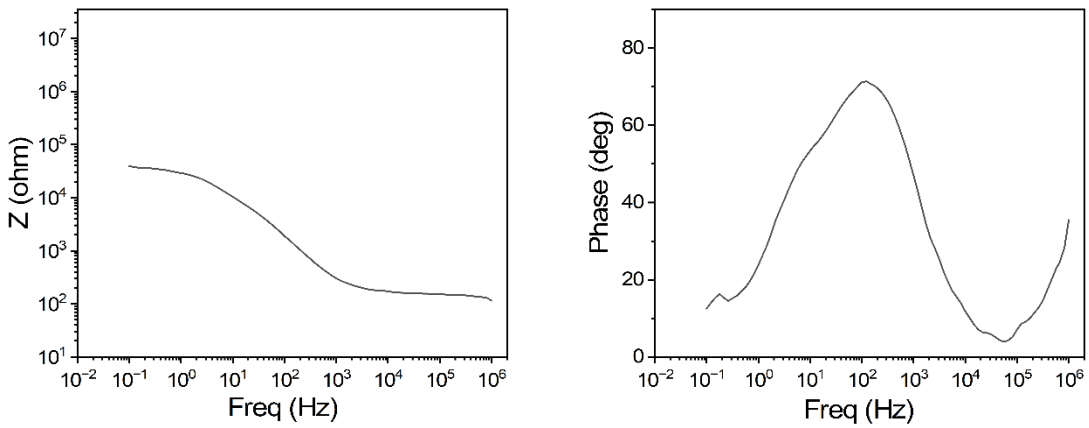

Figure S16 EIS test of the bare electrode at -0.85V vs. Ag/AgCl

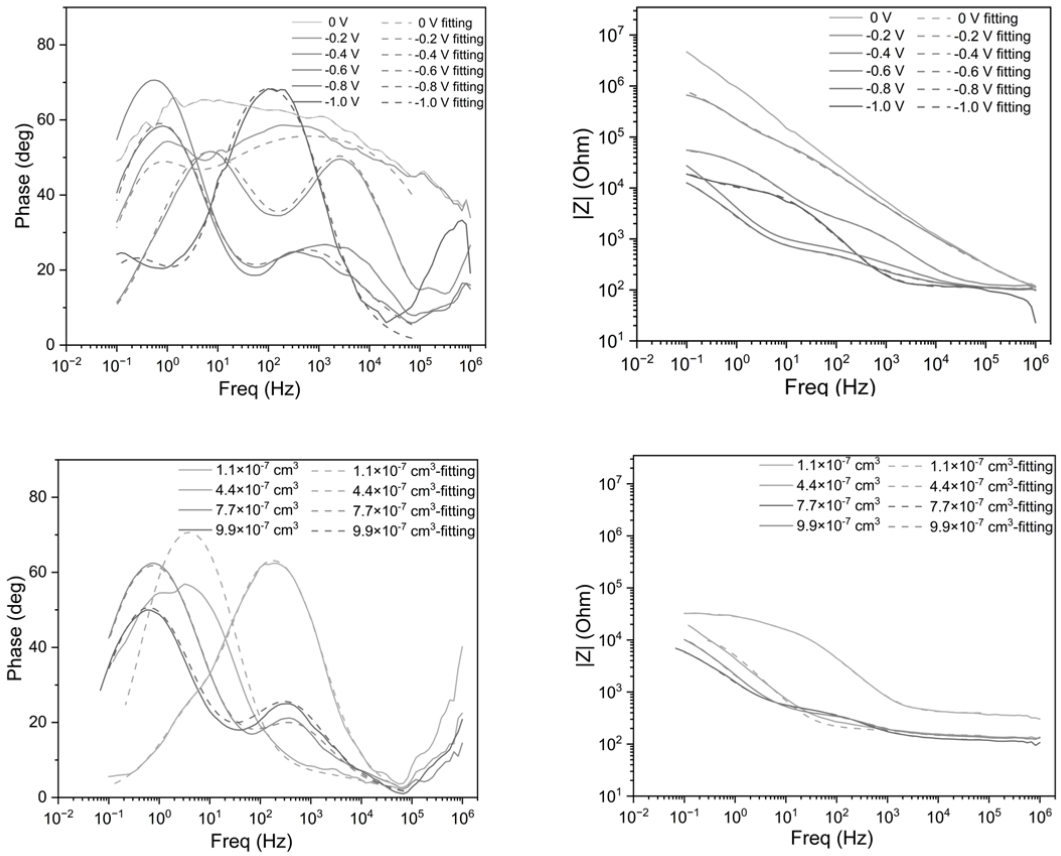

Figure S17 EIS fitting of Volumetric capacitance of different voltage(above) and volumetric capacitance of varying volume(below) of P-3O at 37kDa

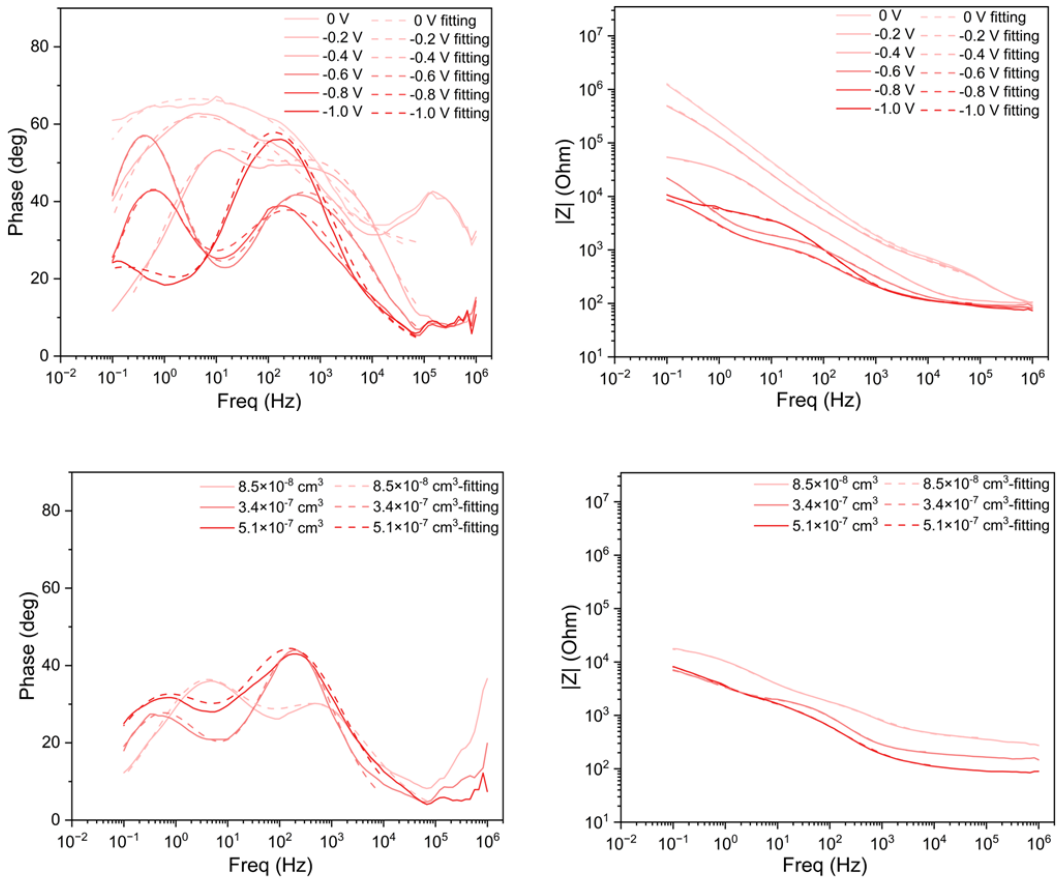

Figure S18 EIS fitting of Volumetric capacitance of different voltage(above) and volumetric capacitance of varying volume(below) of P-3O at 43kDa

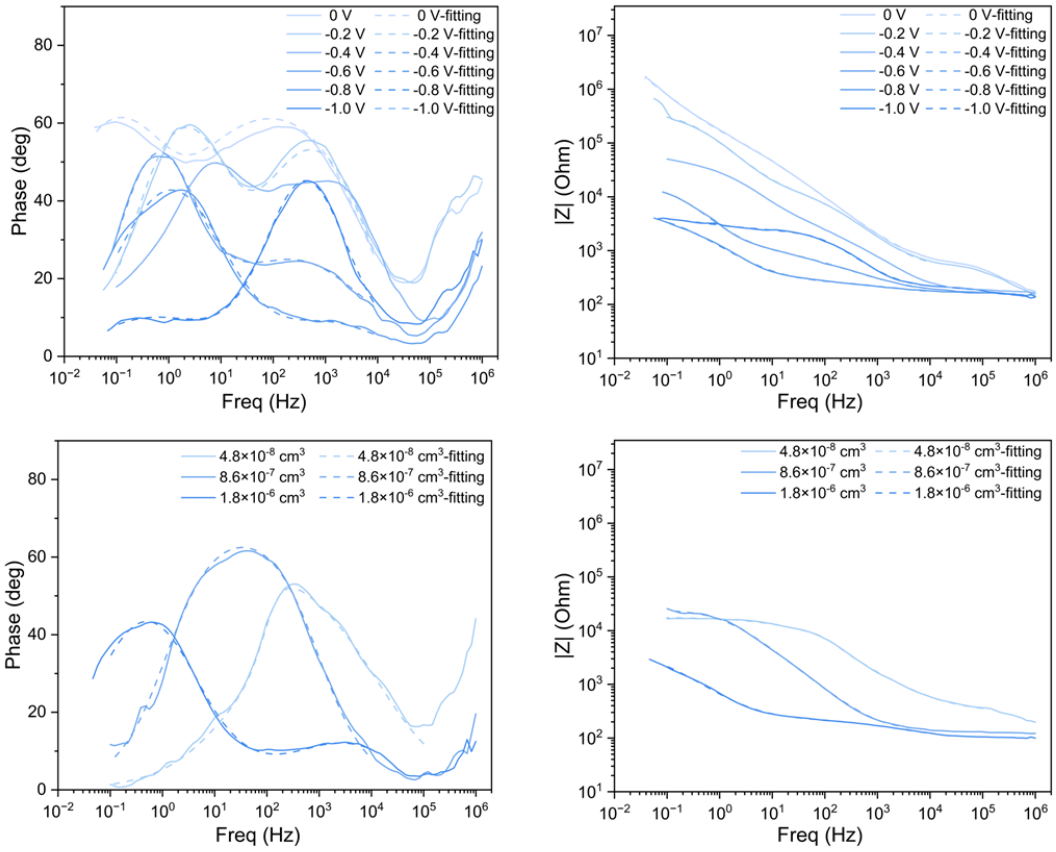

Figure S19 EIS fitting of Volumetric capacitance of different voltage(above) and volumetric capacitance of varying volume(below) of P-3O at 68kDa

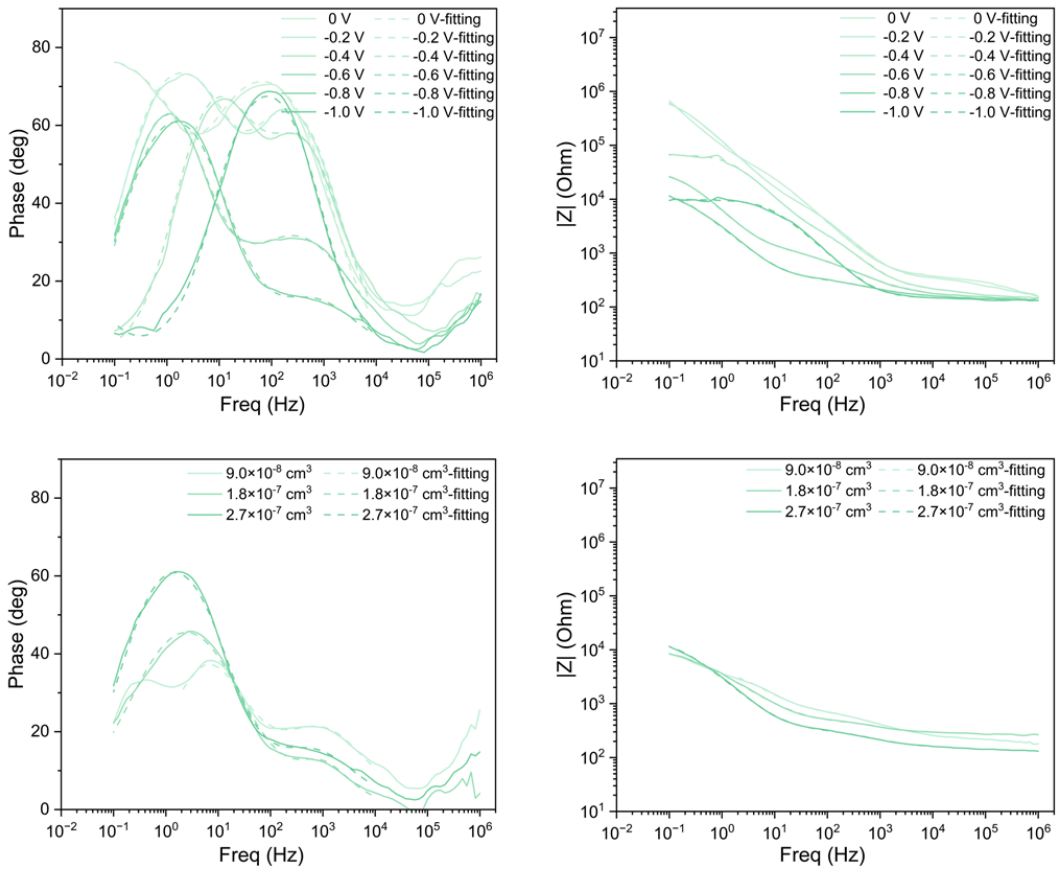

Figure S20 EIS fitting of Volumetric capacitance of different voltage(above) and volumetric capacitance of varying volume(below) of P-3O at 79kDa

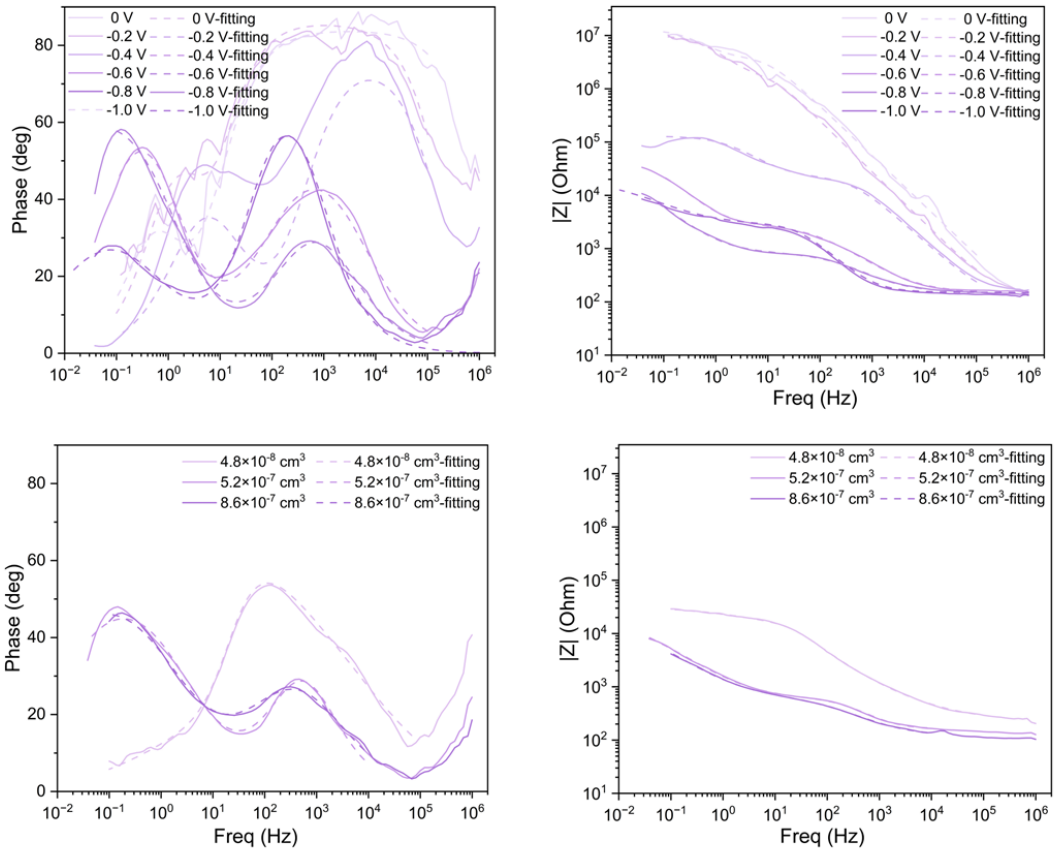

Figure S21. EIS fitting of Volumetric capacitance of different voltage(above) and volumetric capacitance of varying volume(below) of P-3O at 81kDa

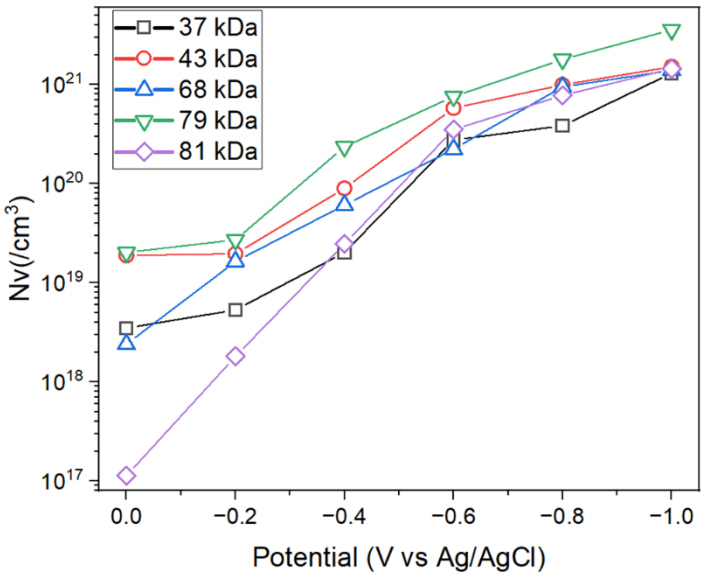

Figure S22 Integral of i-t to calculate charge density of different voltage

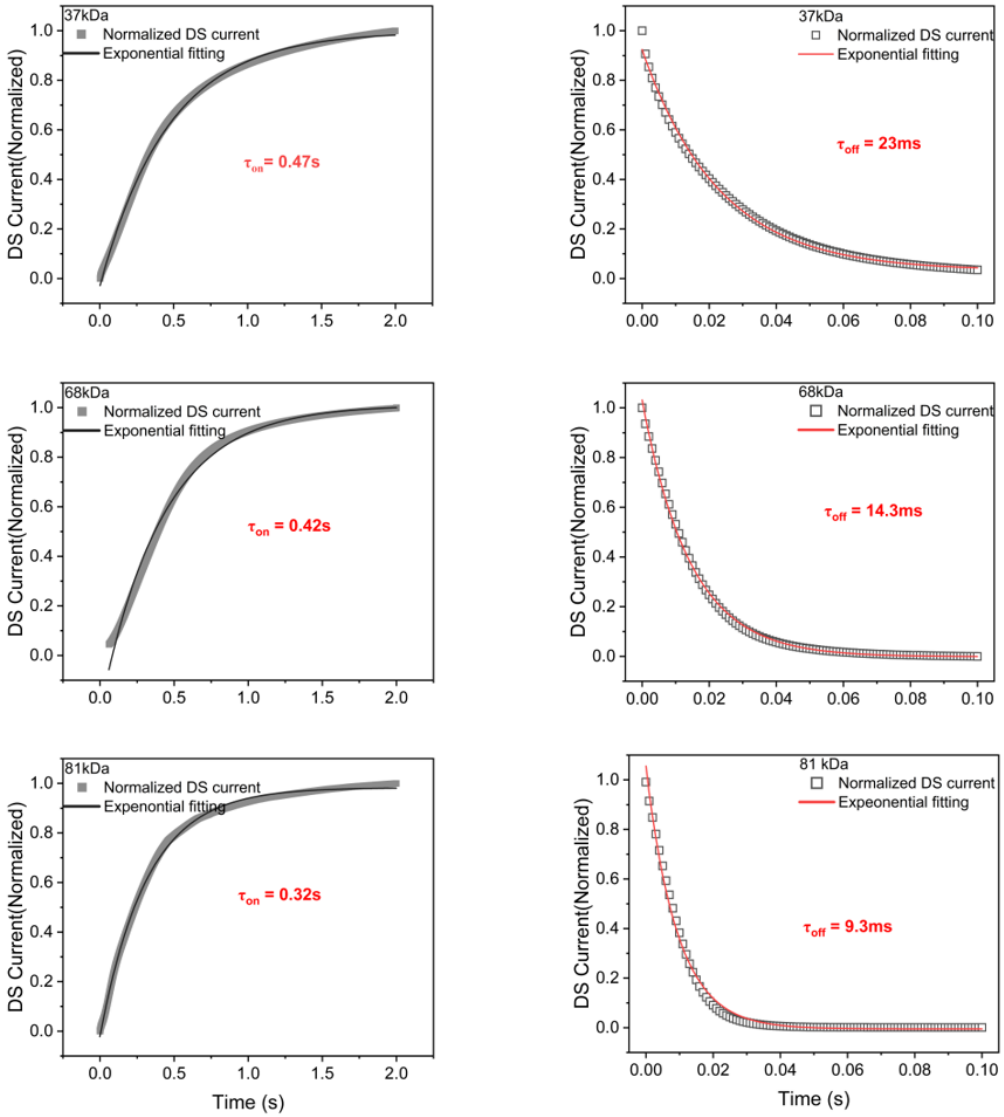

Figure S23 Switch-on and switch-off time of P-3O with Mw = 37, 68, 81 kDa

Reference

1. J. Liu, L. Qiu, R. Alessandri, X. Qiu, G. Portale, J. Dong, W. Talsma, G. Ye, A. A. Sengrian, P. C. T. Souza, M. A. Loi, R. C. Chiechi, S. J. Marrink, J. C. Hummelen and L. J. A. Koster, *Adv. Mater.*, 2018, **30**.
2. P. Pingel, R. Schwarzl and D. Neher, *Appl. Phys. Lett.*, 2012, **100**.